Statistics on High Resolution urban polarimetric images: Application to segmentation and classification.

Nicolas Trouvé, Maxime Sangnier, Elise Colin Koeniguer
ONERA, France

Abstract

In the field of polarimetric, interferometric, or multivariate SAR image segmentation or classification, statistical models are used to design equality test or similarity measure. In this work we address the impact of the choice of various non gaussian models on the final performance in classification or segmentation of urban polarimetric SAR images. As more parameters are used in the description of the distribution, more estimation errors are introduced. It yields that the most complex distribution performance can often be outmatched by simpler models, even in very high resolution or urban settings. As the clutter distribution evolves from gaussian noise to an impulsive non gaussian distribution, there is a breaking point at which using a non gaussian model really becomes beneficial performance wise. In this paper we present preliminary results and methods to improve the choice of an appropriate signal model for a given polarimetric SAR image.

1 Introduction

Nowadays, because of the ever improving image resolution, urban scenario can be studied with the precision required to preserve the small scatterers and spatial features in the images. In the past decade the high resolution sensors motivated the application of numerous non gaussian models under the assumption that the central limit theorem was no longer applicable. While probably true, that assumption does not necessarily mean that non gaussian models will yield improved performance over gaussian traditional models. It may come from the following reasons:

- Spatial heterogeneity is often confused with non Gaussian clutter. Because of the high dynamics and numerous buildings, roads, or sharp edges, traditional methods involving sliding windows usually greatly overestimate the impulsivity of the distribution met in the image.
- As the spatial features in urban scene are very thin, spatial averaging required for the estimation process of the distribution parameters cannot be too large or spatial information will be lost. When few samples are available, multi parameter models tend to behave poorly as the estimation process and parameter variance highly depends on the number of samples.
- The contrast between two areas of the image is not necessarily contained into the high order or shape parameters of the distribution. When the distribution is close to a gaussian distribution, estimating numerous irrelevant parameters actually adds noise to the similarity measures.

In this paper we are interested in the performance of similarity measure used in multivariate SAR image classification or segmentation such as [1], [2], [3]. In the first section we will quickly remind the well known Pearson fields in log-cumulants or second kind cumulants that has been used in many papers to motivate the use of specific non gaussian distributions. In a second time we will show how sliding windows cumulants estimation can be erroneous in case of high spatial heterogeneity as in urban settings. Then we propose a segmentation method of the Pearson field that shows at which point a non gaussian model yields better performance than gaussian model. An application to a SIRV textured clutter will be shown.

2 Compound model and Pearson fields

Most of the models used in the literature to describe non gaussian SAR clutter are using the compound or texture model, assuming fully developed speckle and non-stationarity of the surfaces. In this model the polarimetric clutter is modelled by the product of a zero mean gaussian multivariate complex vector and the square root of a positive texture whose distribution is chosen among the most widely used distribution such as Beta, Inverse Beta, Gamma, Inverse Gamma, Fisher or Weibull distributions. When the intensity of the scattering wave is considered, it yields the product of two positive distributions, the texture and the intensity distribution of the gaussian clutter which depends on the signal dimension. In order to study the texture distribution, the second kind statistics introduced by J.-M. Nicolas in [4], are extremely convenient as the log-moments and log-cumulants allow to obtain the texture statistics by subtracting the gaussian contribution.

Hence, most of the work based on non gaussian models has been motivated by studying the log-cumulants of the

scattered signals over various SAR images. A simple and easy-to-use visual interpretation of the log-cumulants has been introduced in [4] and has been referred as Pearson Diagram. The main advantage of the Pearson diagram is that it provides an initial segmentation of the second and third log-moments κ_2 and κ_3 and can describe most of the widely used texture models. It yields that it is nowadays the most widely used tool to justify a particular choice of texture model. An example of a Pearson fields diagram is displayed on Figure 1. While this tool is a simple and efficient method to analyse a SAR image texture statistic, there are few issues that can arise from the estimation process and the conclusions that are made from this representation.

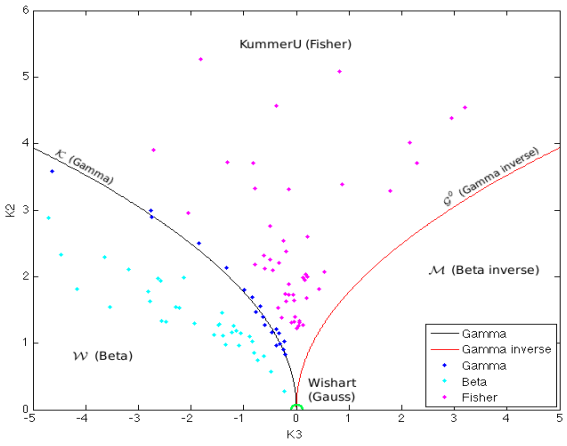

Figure 1: Pearson field and associated texture model.

As it can be seen on Figure 1 the (κ_3, κ_2) space can be divided into subspaces corresponding to specific distribution domains such as Pearson VI, Pearson I, that can be modeled by specific models such as Fisher or Beta distributions. For most users, observing a majority of pixels in a specific area is enough to justify the choice of the associated model. However, it should be done more carefully for the following reasons:

- κ_2 and κ_3 must be estimated. Conclusions depend on their estimation; a careful estimation process must be performed for an accurate conclusion regarding model choice. We will investigate that issue in the third section.

- The space described by the distribution domain means that the estimated shape parameters $\hat{L}, \hat{M}, \hat{\mu}$ associated to the distribution can be computed (i.e, the resulting equation systems have solution), but it does not mean that the performance associated with the whole similarity measure process which involve the estimation of numerous parameters will outpace other models. This effect will be illustrated in the last section.

3 Sliding windows and Cumulants estimation

As most parameters in SAR statistics such as coherency matrices, log-cumulants are estimated and require multiple samples. As they are related to shape parameter, they usually require a large amount of samples for a precise estimation. Usually, they are estimated using the classical sliding windows over the whole image or a section of the image as in [3] and [8]. The problem arises when applied to urban SAR image, when the setting involves numerous sharp edge area transitions, such as building edges, shadows, roads. When a sliding window is applied, it can result in a mixture between two homogeneous areas. Even if those areas are perfectly gaussian distributed, the $\hat{\kappa_2}$ and $\hat{\kappa_3}$ parameters will be overestimated.

In order to illustrate that effect, we will provide an example for a simulated urban SAR scene (using a commercial SAR simulator MOCEM) and from a high resolution polarimetric SAR image from X-band RAMSES sensor. For both images, a 11x11 windows is sliding over a line crossing multiple buildings and various spatial features. We display first on Figure 2 the result of the $(\hat{\kappa_2}, \hat{\kappa_3})$ estimation from the sliding windows over a simulated SAR scene. In this example, the contribution from the gaussian cumulant is removed from the parameters. That means that for gaussian areas, the cumulant should be close to $(0, 0)$. The simulated SAR scene is generated using only gaussian texture as materials (concrete, bare ground) in order to illustrate the effects of the sliding window.

As we can see from the simulated SAR scene, the multiple transitions between two distinct homogeneous areas lead to an overestimation of the parameters, even when the buildings are well separated. Once the sliding windows only contain a single homogeneous area, the estimated parameters quickly fall back to gaussian levels as expected from the chosen texture.

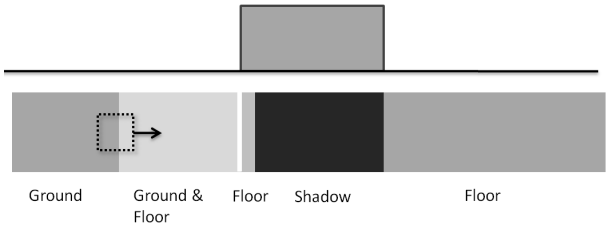

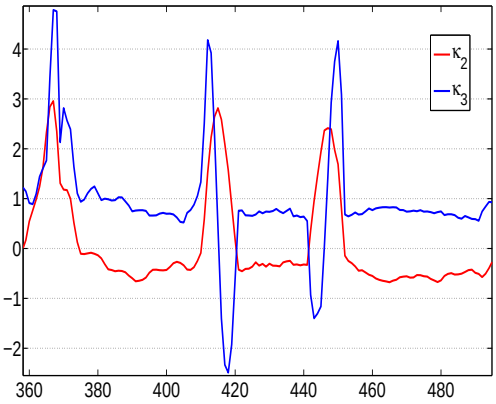

Figure 2: $\hat{\kappa_2}, \hat{\kappa_3}$ parameters for a sliding windows over simulated building SAR scene using gaussian material models

Figure 3 displays the same sliding window estimation over a real SAR image, illustrated above. We can observe the same behavior and the similar value range of $\hat{\kappa_2}, \hat{\kappa_3}$ as for the simulated SAR scene.

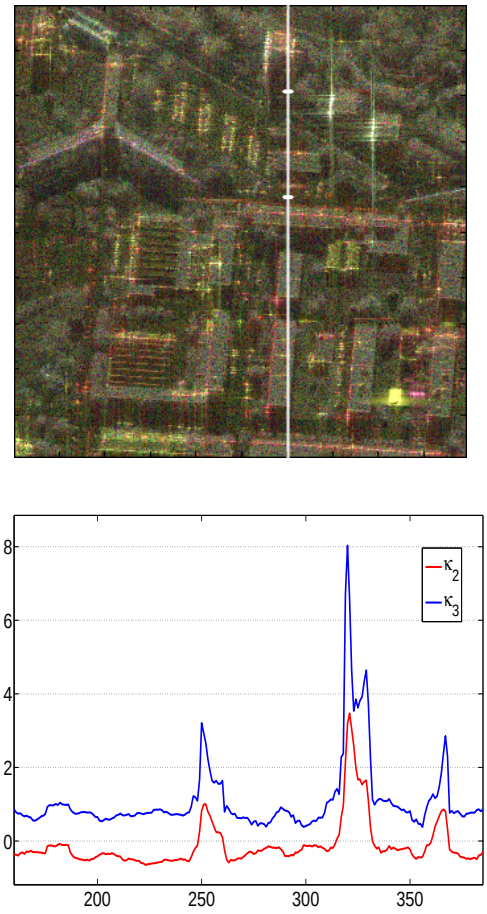

Figure 3: $\hat{\kappa_2}, \hat{\kappa_3}$ parameters for a sliding windows over real SAR scene and polarimetric colored view of the scene and the line along which the estimation is performed.

From those two examples we can conclude that using spatial averaging to estimate the $\hat{\kappa_2}$ and $\hat{\kappa_3}$ parameters in an urban settings is likely to yield much higher absolute values of the parameters and may lead to an inappropriate choice of texture model. Using a handmade or automated partial segmentation of the image for the estimation of the parameters, or accounting for that overestimation will allow a more accurate choice of distribution.

4 Pearson field segmentation

From now on we assume that the log-cumulant analysis has been properly performed and the estimated parameters, even if approximate, are not biased by edges or geometrical effects. It means that we consider that when $\hat{\kappa_2}$ and $\hat{\kappa_3}$ are not null we really have a non gaussian distributed clutter. In this section we will show how gaussian model based similarity measure can outperform a non gaussian similarity measure, even when the clutter is not gaussian. Because the estimation requires several parameters, a limited number of samples can reduce performance, specially for complex distribution models. As the literal expression of the statistic of the test if probably out of reach for non-asymptotic number of samples, the study is performed numerically. The process is done as follows:

- A given couple of (κ_2, κ_3) is fixed. Depending on their region in the Pearson plan, the according distribution is chosen (for our example Beta distribution or Fisher distribution). Using the log-cumulant estimation equations from [5] the "true" associated parameters are computed.
- Given those parameters, three groups of N samples are generated according to the texture distribution and its parameters using the compound model. The first two groups of samples are generated under the H_0 hypothesis, considering the two groups of samples share the same distribution. They are generated using the same texture parameter and the same polarimetric information contained in the coherency matrix of the speckle. A third group of samples are generated under the H_1 hypothesis using the same texture distribution, but another polarimetric coherency matrix. All the coherency matrices used in the simulation have the same total power (SPAN), and all texture distribution have the same scale parameter μ.
- A large number of those three sample groups are generated (10^6 samples for a $P_{fa} = 10^{-2}$). The similarity measures are computed between the first two groups of samples, and allow us to estimate a threshold for a given false alarm probability. Then using one of the two first and the third group the similarity measure under H_1 hypothesis are computed and allow us to compute the detection (or good classification) probability.

- Different similarity measures based on various texture models can be computed that way and allow us, for a given position in the Pearson field, to determine which model yields the best classification performance for the given amount of samples N and the given false alarm probability.

In this paper two similarity measure models are compared. During the conference presentation more model-derived similarity measure will be presented. The first one is the gaussian traditional based similarity measure, which has many names in the literature: Wishart distance , Bartlett distance , or Bhattacharyya distance [1], [7]. It is compared to a SIRV based similarity measure based on the deterministic texture distribution model as presented in [2]. In this example texture is viewed as a perturbation of the polarimetric information. Another part of our work will be dedicated to texture contrast. The Figure 4 shows the result of the segmentation in the beta and fisher distribution area. Red dots correspond to position for which the gaussian distribution similarity measure yields better detection probability. Dots are blue for the SIRV based similarity measure.

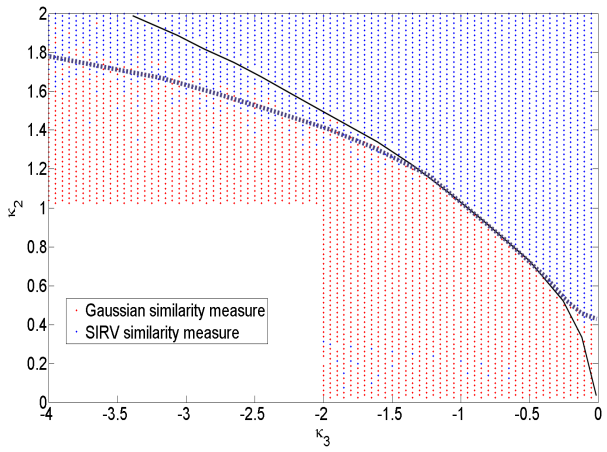

Figure 4: Segmentation of the Pearson field according to classification performance of gaussian versus SIRV similarity measure in the Fisher and Beta region.

From that example we can conclude the following points:

- The performances of the gaussian similarity measure remains good for a large part of the region belonging to Pearson I solutions such as the Beta distribution
- In the Pearson IV region the gaussian model performance decrease quickly especially when the κ_3 moment lies in the $[-0.1; 0]$ interval.
- Nevertheless we can see that there is a not negligeable region in the Pearson IV area in which the gaussian model still outperform the SIRV based non gaussian model.

5 Conclusion

In this paper we have shown preliminary results in improving the accuracy of an appropriate model choice for a given urban SAR scene. The widely used Pearson Field can be improved by a more careful estimation of the log cumulants κ_2 and κ_3. We proposed a mean to segment the Pearson field in regions for which a given model yields the best detection probability for a given false alarm probability and fixed number of samples. During the conference a more detailed version of the segmentation involving a comparison of the Fisher, Beta, SIRV and gaussian model will be presented.

The authors would like to thank the RIM team (ONERA) for providing the airborne RAMSES polarimetric images. They would like to thank also Christian Cochin from DGA for providing the software MOCEM and for its cooperation, patience, and support.

References

[1] Lee, J.S. and Grunes, M.R. and Ainsworth, T.L. and Du, L.J. and Schuler, D.L. and Cloude, S.R. *Unsupervised classification using polarimetric decomposition and the complex Wishart classifier* Geoscience and Remote Sensing, IEEE Transactions 1999

[2] Vasile, G. and Ovarlez, J.P. and Pascal, F. and Tison, C. *Coherency matrix estimation of heterogeneous clutter in high-resolution polarimetric SAR images* Geoscience and Remote Sensing, IEEE Transactions 2010

[3] L. Bombrun and J.-M. Beaulieu. *Fisher Distribution for Texture Modeling of Polarimetric SAR Data*. IEEE TGRS, 5(3), 2008.

[4] J.-M. Nicolas. *Introduction aux statistiques de deuxième espèce : Application des logs-moments et des logs-cumulants à l'analyse des lois d'images RADAR*. Traitement du Signal, 19(3) :139?167, 2002.

[5] J.-M. Nicolas. *Application de la transformée de Mellin: étude des lois statistiques de l'imagerie cohérente*. Note 2006D010, Telecom ParisTech, 2006.

[6] L. Bombrun, S.N. Anfinsen, and O. Harant. *A complete coverage of log-cumulant space in terms of distributions for polarimetric SAR Data*. POLINSAR, 2011.

[7] J.-M. Beaulieu and R. Touzi. *Segmentation of textured polarimetric SAR scenes by likelihood approximation*. IEEE TGRS, 42(10), 2004.

[8] C. Tison, J.-M. Nicolas, F. Tupin, and H. Maître. *A new statistical model for markovian classification of urban areas in high-resolution sar images*. IEEE TGRS, 42(10), 2004.